Available online at www.sciencedirect.com
ScienceDirect
Catalysis Today 127 (2007) 246–255
CATALYSIS TODAY
www.elsevier.com/locate/cattod

Sustainable hydrogen production via reforming of ethylene glycol using a novel spouted bed reactor

Panagiotis N. Kechagiopoulos [a,*], Spyros S. Voutetakis [b], Angeliki A. Lemonidou [a], Iacovos A. Vasalos [b]

[a] Department of Chemical Engineering, Aristotle University of Thessaloniki, P.O. Box 1517, University City, Thessaloniki 54124, Greece
[b] Chemical Process Engineering Research Institute, Centre for Research and Technology Hellas, P.O. Box 361, GR 57001, Thermi, Thessaloniki, Greece

Available online 5 July 2007

Abstract

Hydrogen produced from renewable energy sources is of great interest as an alternative to fossil fuels and as a means for clean power generation via fuel cells. The aqueous fraction of bio-oil can be effectively reformed to hydrogen rich streams in the presence of active catalytic materials. In this paper we present the experimental work carried out in a novel spouted bed reactor for the reforming of bio-oil. The use of a specially designed injection nozzle in combination with the particular hydrodynamic characteristics of the spouted bed resulted in efficient processing of the organic feed. The known problem of coking was notably avoided regardless of the loading material of the reactor. The effect of reaction temperature and steam to carbon ratio in the feed was investigated in the presence of various catalytic and non-catalytic particles. Runs were conducted with ethylene glycol as a representative model compound of the aqueous phase of bio-oil. Olivine, when associated with nickel, proved to be a very suitable catalytic material for the process combining high activity in reforming, anti-coking characteristics combined with exceptional mechanical strength.

Keywords: Hydrogen; Bio-oil; Reforming; Ethylene glycol; Spouted bed reactor; Ni/olivine catalyst

1. Introduction

Pollution of the environment due to the use of conventional fuels, in conjunction with the concern for the depletion of oil reserves, necessitates the intensification of research for alternative energy sources. Hydrogen is emerging as the energy carrier of the future since it can be used as a clean transport fuel as well as a means for the production of electricity via fuel cells. It is thus appearing as an attractive selection for sustainable development. Currently, hydrogen is mainly produced from non-renewable sources, namely natural gas and petroleum fractions [1], leading to high CO_2-emissions and significantly contributing to the greenhouse effect. Hydrogen can present environmental benefits only when derived from renewable energy sources, such as biomass, however processes like biomass gasification and pyrolysis are not mature enough for commercialization. Steam reforming of pyrolysis oil (bio-oil) is one of the promising routes of sustainable hydrogen production. Bio-oil, a product of biomass pyrolysis, can be separated with addition of water into a hydrophobic lignin derived fraction and an aqueous fraction (~50% of bio-oil) containing mostly the carbohydrate-derived monomeric compounds at a ratio of ~20% organics/~80% water [2,3].

Pyrolytic lignin is a valuable material, which can be used to produce different chemicals and additives [4,5], whereas the aqueous fraction can be steam reformed for hydrogen production. This integrated approach presents certain advantages compared to other hydrogen production processes from biomass, such as biomass gasification. Bio-oil being a liquid is a lot easier to transport and handle compared to bulky solid biomass. Consequently the steps of pyrolysis and reforming can occur at different sites. Biomass pyrolysis could take place near agriculture cultivation, while hydrogen could be produced at the site of power generation or near the existing infrastructure for hydrogen use. Moreover, the fact that the aqueous phase of bio-oil contains ~80% of water reduces significantly the use of additional water necessary for the steam reforming reaction.

* Corresponding author. Tel.: +30 2310 498318; fax: +30 2310 498380.
E-mail address: kechagio@cperi.certh.gr (P.N. Kechagiopoulos).

0920-5861/$ – see front matter © 2007 Elsevier B.V. All rights reserved.
doi:10.1016/j.cattod.2007.05.018

The co-reforming of pyrolysis liquids with other bio-based gases containing methane, e.g. landfill gas or anaerobic digester gas (biogas) [6] could further increase hydrogen production in a biomass-based plant.

The catalytic reforming of the water soluble fraction of biomass pyrolysis liquids was studied extensively in our previous publication employing a pilot scale fixed bed reactor [7]. Representative model compounds (acetone, ethylene glycol and acetic acid) were reformed effectively in the presence of a commercial nickel-based catalyst. Hydrogen yields up to 90% were achieved at reaction temperatures higher than 600 °C and H_2O/C ratios higher than 3 with complete conversion of the organics. On the contrary, reforming of the aqueous phase of bio-oil resulted in a much lower hydrogen yield around 60% due to the high extent of coking. The majority of available publications in this field have focused on the reforming of model compounds, predominantly acetic acid [8–14], while a smaller number of researchers have also studied real bio-oil or its aqueous phase [15–19]. The major problem of coke deposition led Chornet and co-workers [15] to suggest the use of fluidized bed as more suitable for the reforming of bio-oil, while Davidian et al. [19] proposed a sequential process alternating between cracking/reforming and combustion steps. An alternative approach was introduced by Dumesic et al. [20–22], where hydrogen is produced by aqueous-phase-reforming (APR) of biomass derived oxygenated molecules (e.g. ethylene glycol, glycerol, sorbitol). Low temperatures (∼200 °C) and high pressures (∼25 bar) are used, making it possible to generate hydrogen with low amounts of CO in a single chemical reactor. It is clear that the successful development of the process largely lies in the design of a proper reactor in conjunction with active catalytic materials.

Previous work relating to biomass gasification [23–25] has shown that natural olivine (an iron and magnesium orthosilicate) can be an appropriate fluidized bed material because of its hardness and its catalytic activity, mainly due to the iron it contains. Courson et al. [26] enhanced olivine performance by developing a Ni/olivine catalyst that was tested for the reforming of methane [27,28] in a laboratory scale unit. The reported activity and stability (attrition and carbon-deposition resistance) of the catalyst was attributed to strong Ni/olivine interactions developed during calcination.

An alternative reactor configuration that has not yet been employed in the reforming of bio-oil is the spouted bed reactor. This particular type of reactor presents certain advantages when compared to conventional fluidized beds that are well recognized in literature [29]. The gas phase is characterized by very short residence times, while the mixing of the catalytic particles is almost perfect. Additionally, the cyclic movement of the solids allows for very efficient heat recirculation. The reactor presents low-pressure drop, is relatively easy to scale up and has great versatility in handling a wide range of particle sizes and gas velocities. These features could be very beneficial to the reforming of the unstable oxygenates contained in bio-oil.

In the current work, we present the experimental results of reforming of ethylene glycol using a pilot scale spouted bed reactor. The use of a specially designed injection nozzle allows the direct atomization and contact of the liquids with the catalyst particles. Primary aim of the work was to validate the suitability of the reactor in handling liquid feedstocks. Various catalytic and non-catalytic particles were tested with Ni/olivine exhibiting very promising performance and high resistance to attrition.

2. Experimental

2.1. Materials and preparation

All particles, catalytic and non-catalytic, investigated were sieved in order to get a particle size of 250–355 μm. Thermal decomposition reactions were studied using inert sand (SiO_2). Natural olivine, provided from Olivinites Macedonia Greece, was used as the support for nickel as well as a standalone loading material of the bed. Its composition corresponds to a mean formula $(Mg_{0.9}Fe_{0.1})_2SiO_4$, containing also small quantities of $MgSiO_3$ and iron oxides, as well as much smaller amounts of Ni and Ca. Prior its use olivine was calcined at 1100 °C for 4 h.

The Ni/olivine catalyst was prepared by wet impregnation of natural olivine with a solution of $Ni(NO_3)_2{\cdot}6H_2O$ in de-ionized water so as to obtain a nickel content of 5 wt%. After water evaporation in a mild vacuum at 95 °C, the samples were dried overnight at 105 °C and then calcined under air for 4 h at 800 °C with a heating rate of 5 °C min^{-1}. Prior testing, catalytic particles were subjected to cold flow spouting (details of cold flow unit given below) to evaluate their resistance to attrition at conditions equivalent to the ones actually faced in the spouted bed reactor. Particles exhibited initially weight losses in the form of fines that appeared at the top of the bed and were removed using a vacuum hood. Attrition interestingly had a limit, after which no more fines were created. The resulting stable particles after cold flow spouting were the ones actually loaded in the reactor during catalytic tests.

2.2. Characterization methods

Specific surface area was determined by the BET-method on a Tristar Micromeritics instrument on the basis of the N_2 physisorption capacity at −196 °C. The crystalline phases of samples were examined by powder X-ray diffraction (XRD) on a Siemens D500 diffractometer using Cu Kα radiation (λ = 1.5406 Å). Synthesized materials were examined by scanning electron microscopy (SEM) on a JEOL 6300 microscope, coupled with X-ray energy dispersive spectroscopy (X-ray EDS, Oxford Link ISIS-2000) for local elemental composition determination. Samples were mounted in epoxy, cut in order to obtain planar sections of the grains, polished and examined by SEM/EDS. Carbon deposits on used samples were examined on a C, H elementary analyzer (LECO-800).

2.3. Experimental unit

A schematic diagram of the SYNGAS pilot plant facility is presented in Fig. 1. The process control of the fully automated unit is based on an industrial computer control system, which is

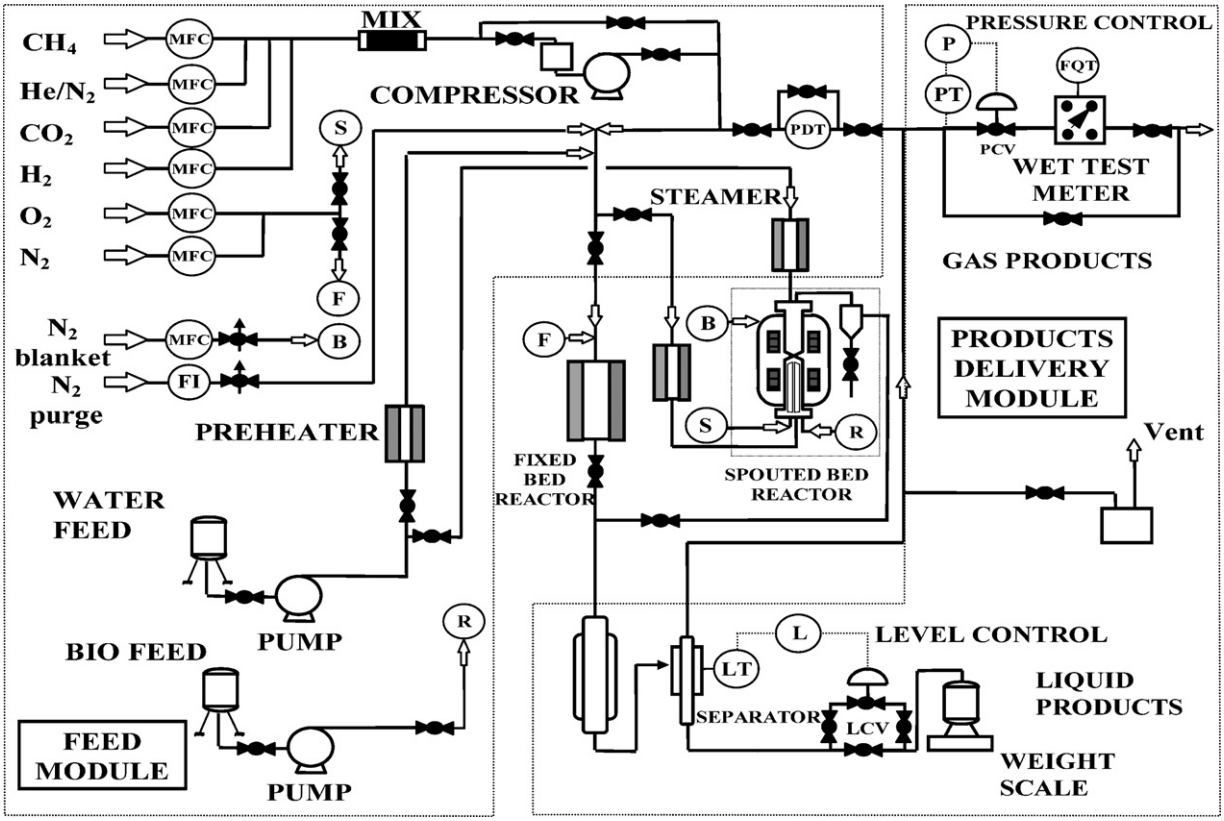

Fig. 1. Simplified flowchart of the SYNGAS pilot plant unit used for the ethylene glycol reforming study.

coordinated by the FIX/MMI software. Since the pilot plant unit has been described previously [7] elaborately, details will be given here only for the spouted bed reactor that is employed for the first time.

The reactor made of stainless steel (Fig. 2) comprises an inverted conical base followed by a cylindrical part (50 mm i.d.). Steam plus the gas feed is admitted to the reactor from the preheater region through a nozzle located at the cone apex. The mixture of steam and gases create a jet that entrains catalyst particles and forms a spout around the reactor centerline. The spout behaves essentially as a dilute phase catalytic transport line, which is surrounded by, and interacts with, the slowly moving annular dense bed through gas and particle exchange currents. A paraboloidal fountain of particles is formed in the freeboard above the bed surface when the jet momentum is high enough to maintain stable spouting. Entrained catalyst particles from the spout region are separated from the product gases in the fountain and fall back to the top of the annular catalyst bed. The organic feed reaches the reactor cooled from a separate line and is subsequently mixed in liquid form with the spouting jet just before the cone apex. Thus, the injected liquid organics come into immediate contact with the particle bed. After leaving the reaction zone, the gas products are quenched by a cooling coil surrounding the exit of the reactor. Heat is supplied to the reactor by a two-zone furnace surrounding the catalyst bed. The furnace is controlled by thermocouples located outside the reactor while the temperature profile along the catalyst bed is monitored by thermocouples placed inside a thermowell.

2.4. Cold flow studies

Stable spouting occurs over a specific range of gas velocities for a given combination of spouting gas, solid particles and column configuration. As gas velocity increases, transition from static to coherent spouting, bubbling, slugging or simply fluidization takes place [29]. Volumetric flow inside the reactor under operating conditions depends not only on temperature and pressure conditions studied, but also on the conversion achieved. Reforming reactions are usually accompanied by significant volume expansion making it highly important to carefully determine the window of gas velocities for coherent spouting. Cold flow studies were conducted to establish these spouting limits. The unit consists of a transparent spouted-bed column with geometry identical to the actual reactor. The cylindrical part of the column is made out of glass with the cone made of polycarbonate and flanged to the cylinder. Experiments were carried out at atmospheric conditions using silica sand and olivine as bed materials. The spouting gas was air and entered the column through a tube at the apex of the cone.

2.5. Experimental conditions and procedures

The experiments were performed in the spouted bed reactor, using constant pressure (1 bar), while the operating parameters varied were the temperature, H_2O/C ratio in the feed and O_2/C ratio. In the first phase of this study ethylene glycol (99.7%, Prolabo) was selected as a model compound of the aqueous

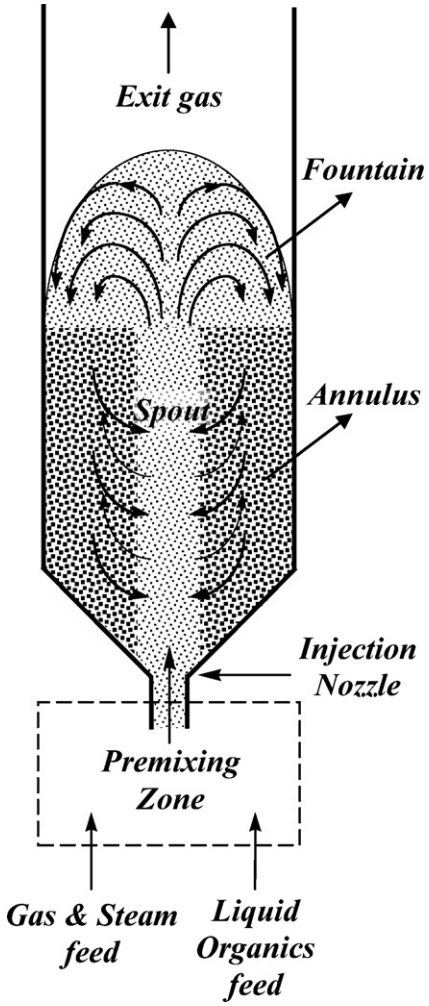

Fig. 2. Schematic diagram of the spouted bed reactor.

phase of bio-oil. The range of experimental conditions used in these sets of experiments is summarized in Table 1.

Constraints imposed by the requirement of acceptable spouting, as determined from cold flow runs, were used to determine the space velocities to be used at reaction conditions. During the initial start up of the experiment nitrogen is admitted to the reactor as a spouting agent. Gradually part of nitrogen flow is replaced by equal volumetric flow of steam and subsequently the liquid organics are fed to the reactor. At any time the sum of reactants and nitrogen flows fed is calculated to be within the spouting limits. The volumetric flow of the reactor exit stream is also continuously monitored to ensure it does not exceed the coherent spouting window.

Table 1
Summary of ethylene glycol reforming experimental conditions

	Sand		Olivine	Ni/olivine
T (°C)	600–850		650–850	650–850
H_2O/C	0	4.6	4.6	4.6
N_2 dilution (vol%)	95	75	65	50
O_2/C	0		0–0.1	0
Feed flow rate (slpm)	8		7	9
Reactor load (g)	140		140	140

An online gas chromatograph (HP 6890) is used for the analysis of gas products. Two columns (PoraplotQ and Molecular Sieve 5A) in series-bypass configuration and two detectors (thermal conductivity and flame ionization) are used for the analysis of gases. Liquid samples collected are analyzed offline in a Varian 3300 gas chromatograph using a FFAP capillary column and a flame ionization detector.

The results presented in the subsequent section are expressed in terms of the following parameters:

Carbon to gas (C-to-gas) conversion:

$$X_{\text{gas}} = \frac{\text{moles of carbon converted to gas products}}{\text{moles of carbon in the feed}} \times 100 \quad (1)$$

Hydrogen yield:

$$H_2 \text{ yield} = \frac{\text{moles of hydrogen obtained}}{2.5 \times \text{moles of carbon fed}} \times 100 \quad (2)$$

Selectivity of hydrogen:

$$S_H(H_2) = \frac{\text{moles of hydrogen obtained}}{\text{moles of hydrogen contained in gas products}} \times 100 \quad (3)$$

Selectivity of x carbon containing gas product:

$$S_C(x) = \frac{\text{moles of carbon converted to } x \text{ compound}}{\text{moles of carbon converted to gas products}} \times 100 \quad (4)$$

Carbon balance closure in all tests was in the order of $100 \pm 5\%$.

3. Results and discussion

The aqueous fraction of bio-oil is a complex mixture of oxygenated compounds, which can be classified in the main categories of acids, alcohols, aldehydes and ketones [9]. The concentration of ethylene glycol in the aqueous phase of bio-oil can reach up to 2% [30]. Apart from that, it can also be considered as a representative compound of the entire alcohol group contained in the aqueous fraction. For ethylene glycol the stoichiometric steam reforming reaction that is given below:

$$C_2H_6O_2 + 2H_2O \rightarrow 2CO_2 + 5H_2 \quad (5)$$

yields 2.5 mol of H_2 per mole of carbon input, representing the highest hydrogen yield that can be derived. On the other hand, production of syngas from ethylene glycol and any other carbohydrate that follows the general formula $C_n(H_2O)_mH_2$ can occur only via direct decomposition [31], as seen in reaction (6):

$$C_2H_6O_2 \rightarrow 2CO + 3H_2 \quad (6)$$

The yield of hydrogen is always lower than the stoichiometric maximum achieved via reaction (5), because two undesirable products, CO and CH_4, are also formed via the water gas shift (7) and methanation (8) reactions:

$$CO + H_2O \rightleftarrows CO_2 + H_2 \quad (7)$$

$$CO + 3H_2 \rightleftarrows CH_4 + H_2O \quad (8)$$

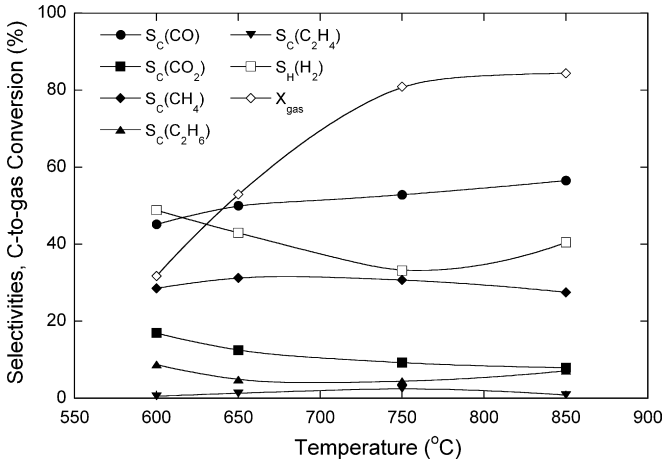

Fig. 3. Ethylene glycol conversion to gas products and their selectivities vs. temperature using silica sand as a loading material ($H_2O/C = 4.6$).

3.1. Performance of silica sand

Thermal decomposition of the organic compounds contained in the bio-oil can be a very important factor in the performance of the process. Coking not only leads to lower hydrogen yields, but also causes severe catalyst deactivation and reactor blockage. Many of these compounds are thermally unstable at the temperatures required for steam reforming, so that the steam reforming competes with thermal decomposition reactions:

$$C_nH_mO_k \rightarrow C_xH_yO_z + \text{gas}\,(H_2,\ CO,\ CO_2,\ CH_4,\ \ldots) + \text{coke} \quad (9)$$

It can be understood from the above that the study of thermal decomposition of ethylene glycol in the spouted bed reactor is of great interest since useful information can be derived concerning its suitability in the particular process. Silica sand (SiO_2) is completely inert and is therefore a proper loading material acting merely as a heat carrier. Runs were conducted in the absence and presence of steam. In the entire range of conditions studied, the main gaseous products were CO, CO_2, CH_4, H_2, C_2H_6 with smaller amounts of C_2H_4 (Fig. 3). The presence of steam did not seem to influence noticeably the selectivity of gaseous products or the total conversion, proving that ethylene glycol is thermally decomposed in the presence of SiO_2. In Table 2 we compare the selectivities of carbon containing compounds plus the conversion of ethylene glycol to gases at 850 °C under the presence and absence of steam. Apart from a slightly higher participation of the water gas shift reaction under the presence of steam, as indicated by the respective CO and CO_2 selectivities, no other important differences can be observed. Thus, the discussion that follows refers actually to either case as far as gas composition and carbon to gas conversion is concerned. Increase of temperature from 600 to 850 °C led to an increase of ethylene glycol conversion to gases from 32 to 85%, as seen in Fig. 3, with the remaining percentage detected in the liquid products either as unconverted ethylene glycol or as acetaldehyde (mainly), acetone, methanol, ethanol and acetic acid that were produced from the various thermal reactions. Acetaldehyde, the main liquid product in these runs, was also detected by Dauenhauer et al. [31], who studied the autothermal steam reforming of ethylene glycol. Its formation was attributed to the homogeneous dehydration of ethylene glycol according to the following reaction:

$$C_2H_6O_2 \rightarrow C_2H_4O + H_2O \quad (10)$$

Water was detected in liquid samples collected from runs in the absence of steam, indicating the presence of the above reaction. The subsequent decarbonylation of acetaldehyde leads to methane explaining partly its high percentage in the gas products:

$$C_2H_4O \rightarrow CH_4 + CO \quad (11)$$

Hydrogen selectivity was low, fluctuating below 50% with the highest percentage lost bound in CH_4 and the liquid compounds produced. The direct decomposition of ethylene glycol (reaction (6)) is most likely responsible for the produced H_2.

The effect of temperature on gas product composition is not particularly strong (Fig. 3). Apart from the change in carbon to gas conversion, the selectivities of gas products remain roughly stable. The most important conclusion deducted from this set of experiments concerned coking. Even though thermal decomposition reactions clearly dominated and thermodynamically the production of coke is possible at these conditions [32], carbonaceous deposits were especially limited demonstrating the rapid and effective mixing between the hot solid particles and the cold injected reactants. The very short residence time of reactants seems to be beneficial in suppressing reactions that lead to coke. The organics after atomization come into immediate contact with the hot particles, decompose rapidly to various gaseous compounds and exit the reactor. As a result, coke deposits did not exceed 0.15 wt% of the sand bed amounting to less than 1% of carbon contained in ethylene glycol.

Table 2
Comparison of gas products selectivities and C-to-gas conversion under the presence and absence of steam ($T = 850$ °C, $H_2O/C = 4.6$, loading material: silica sand)

	No steam	With steam
$S_C(CO)$	59.73	56.54
$S_C(CH_4)$	26.61	27.52
$S_C(CO_2)$	4.15	7.95
$S_C(C_2H_6)$	8.90	7.15
$S_C(C_2H_4)$	0.61	0.84
$S_H(H_2)$	39.46	40.47
X_{gas}	84.64	84.41

3.2. Performance of olivine

A relative improvement was observed upon loading the reactor with calcined olivine. This mineral, as will be discussed in Section 4, is known to present catalytic action, mainly due to the presence of iron species [24,33,34]. Swierczynski et al. [34]

specifically proposed that reduced Fe is responsible for the activity of olivine. This observation was supported by the fact that the same calcined olivine, showed positive performance in steam gasification under reducing conditions [35], but was not equally active in gasification with air [23]. It was thus decided to carry out all these runs in the presence of steam. The most important difference, observed at similar conditions to the sand experiments, was related to the conversion of ethylene glycol towards gaseous products. As clearly seen upon comparison of Figs. 3 and 4a, a 10–20% increase was brought about in carbon to gas conversion from the use of olivine. At 650 °C, 70% of incoming carbon was converted to gases with this value rising to 95% at 850 °C (Fig. 4a). It was previously demonstrated by Rapagna et al. [35] that olivine promotes cracking of heavy components and from our study we can infer a similar behavior for ethylene glycol.

Apart from the beneficial effect of olivine on conversion of ethylene glycol, the selectivities of gas products were generally similar to sand as depicted in Fig. 4a. The product gas was composed exclusively of CO, CO_2, CH_4, H_2 and C_2H_6. The results suggest once again that decomposition of ethylene glycol is dominant. The high selectivity of methane and ethane in the product stream, suffice to prove the low extent of

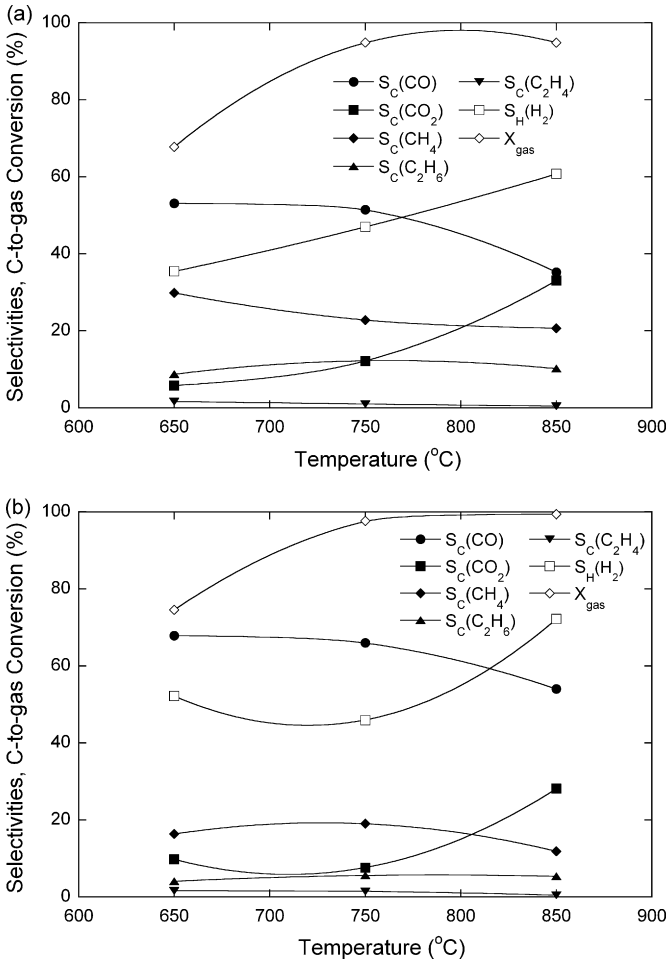

Fig. 4. Ethylene glycol conversion to gas products and their selectivities vs. temperature using calcined olivine as a loading material and (a) $H_2O/C = 4.6$, (b) $H_2O/C = 4.6$, $O_2/C = 0.1$.

reforming reactions. Additionally, the increased selectivity of CO over CO_2 at most temperatures studied implies also the very small extent of the water gas shift reaction. Only at 850 °C did we observe a shift in the composition of gas products that indicated a higher extent of reforming reactions. CO_2 and H_2 selectivity increased and the inverse effect was observed for CO and CH_4 selectivity. Combined with the increased conversion achieved at this temperature, these favorable selectivities resulted in the highest hydrogen yield for these runs. On the other hand, coke deposition on olivine was equally low compared to sand averaging at 0.15 wt% of the bed for a typical experiment (minimum 5 h TOS), percentage equivalent to 0.5 wt% of the total incoming carbon. GC analysis of liquid products samples collected during different olivine runs revealed additional interesting information. Only traces of ethylene glycol were detected, with acetaldehyde being the only compound at noteworthy concentrations. In other words, conversion to gas and liquid compounds in the presence of olivine was complete for all temperatures, further proving its activity in cracking reactions.

The presence of oxygen in the feed was also examined. As explained previously, nitrogen is co-fed with steam in order to adjust the total flow in the reactor and stay within the spouting limits. Part of this nitrogen was replaced by air to achieve an O_2/C ratio equal to 0.1. The resulting selectivities of gaseous products together with C-to-gas conversion are presented in Fig. 4b where we can observe that for temperatures higher than 750 °C total conversion to gases was achieved. If we compare Fig. 4a and b, we can notice the lower selectivity to CH_4 and C_2H_6 imposed by the presence of oxygen. This is attributed to the combustion of these compounds, as also deduced from the respective rise in CO_x selectivities. The complete absence of organic compounds in liquid products above 750 °C further suggests that thermal products of ethylene glycol decomposition are oxidized by oxygen. The most important finding though, was that co-feeding of oxygen at a relatively low percentage, led to complete elimination of carbonaceous deposits.

The effectiveness of olivine as a fluidizable material has been widely recognized in literature [23,25] and indeed from our study its high resistance to attrition was proved. The spouted bed reactor operates at conditions requiring materials with mechanical strength even higher than fluidized beds do, due to the toroidal motion of the particles. Calcined olivine exhibited weight loses due to attrition that did not exceed 1 wt% for a typical experiment (minimum 5 h) demonstrating its suitability for the particular process. The mechanical strength of olivine could easily be compared with that of silica sand, as was also pointed out by Devi et al. [24].

3.3. Performance of Ni/olivine catalyst

Fig. 5 depicts the experimental results obtained in the presence of Ni/olivine catalyst. The differences from the respective runs with olivine and sand are evident. In the entire range of temperatures used, the conversion of ethylene glycol to gaseous products was complete. Close examination of gas

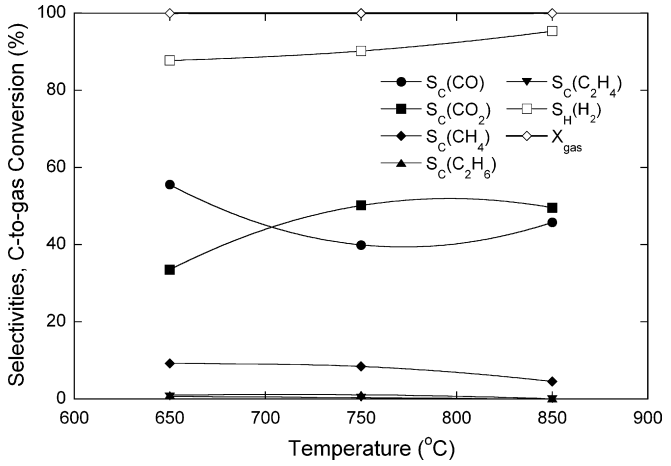

Fig. 5. Ethylene glycol conversion to gas products and their selectivities vs. temperature using Ni/olivine catalyst as a loading material and H_2O/C = 4.6.

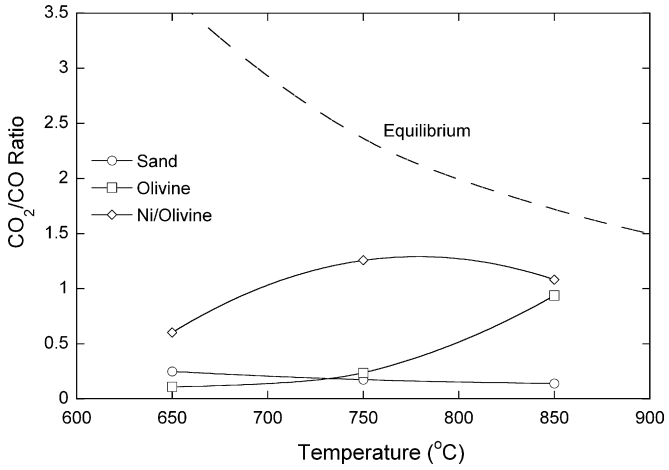

Fig. 6. CO_2/CO ratio vs. temperature for various catalytic and non-catalytic particles tested at H_2O/C = 4.6. Comparison with thermodynamically predicted values.

products selectivities can explain the significant increase in C-to-gas conversion. Selectivity towards C_2H_4 and C_2H_6 is almost zero, whereas in the previous non-catalytic runs an important percentage of carbon was converted to these compounds (especially C_2H_6). More interestingly, selectivity to CH_4 that averaged between 20 and 30% in non-catalytic tests, exhibits also a significant reduction. At 650 °C, 10% of the converted ethylene glycol resulted in CH_4 with this value dropping below 5% at 850 °C. Liquid samples were free of any organic compounds, since conversion to gases was complete. All the above, strongly indicate the activity of the catalyst in reforming reactions. Apart from the small percentage lost in CH_4, ethylene glycol was converted completely to CO_x and H_2. This resulted in high hydrogen selectivity that averaged at 90–95% depending on temperature.

The selectivities of products, especially when compared to non-catalytic ones, can give us insight on the sequence of reactions taking place in the spouted bed reactor. CH_4 detected during catalytic runs is most probably an intermediate product of decomposition reactions. Methanation (reaction (8)) leading to CH_4 from H_2 and CO cannot explain the high CH_4 percentage in the exit stream, since this exothermic reaction is not favored thermodynamically at the temperature range studied [36]. Thermal reactions and catalytic reforming reactions take place simultaneously and in a way antagonize. Part of ethylene glycol decomposes thermally, while the rest is reformed with steam towards H_2 and CO_x. The results obtained are not enough to claim about the parallel and/or consecutive reaction network of reforming and decomposition reactions. Further mechanistic investigations are necessary to elucidate the elementary steps leading to the formation of the final products. However, it is evident that the catalyst is active enough to reform thermal products, such as CH_3CHO, since no traces were detected in the liquid products. Higher hydrocarbons C_2H_4 and C_2H_6 are also totally reformed with CH_4 being the only thermally produced compound that makes it to the gas products. Ni/olivine catalysts have been proved to be effective in methane reforming [26–28], consequently the presence of the later in the reactor exit implies that the concentration of active Ni sites in the present catalyst was not high enough. It should also be pointed out that, since thermal decomposition reactions do occur at some extent, part of CO_x produced are in fact thermal products (via reactions (6) or (11) for example).

Regardless the origin of carbon oxides (thermal or catalytic), insight can be gained on the extent of the water gas shift reaction from their respective ratio since this reaction is equilibrium controlled. In Fig. 6 we compare CO_2/CO ratio versus temperature for the various particles examined with the thermodynamically predicted for equivalent conditions. Sand seems totally inactive in promoting the water gas shift reaction, while olivine shows only a slight activity at 850 °C. The Ni/olivine catalyst appears more active at all temperatures, especially over 750 °C, but still is not at equilibrium. Conclusively, promotion of water gas shift reaction to thermodynamic limits together with full reformation of methane will result in further increase in hydrogen production.

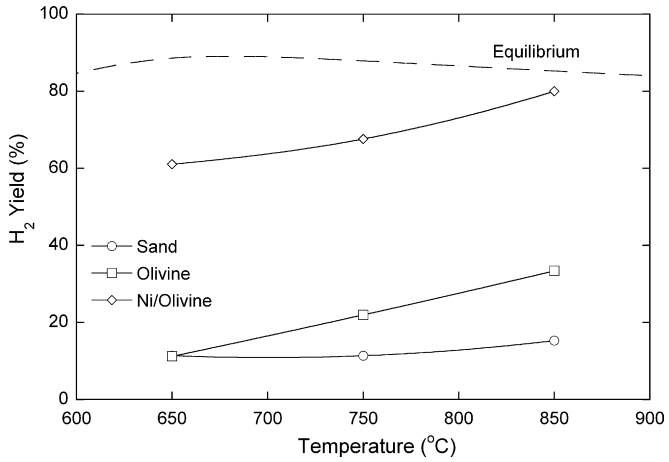

Fig. 7. Hydrogen yield vs. temperature for various catalytic and non-catalytic particles tested at H_2O/C = 4.6. Comparison with thermodynamically predicted values.

This is better illustrated in Fig. 7, where the production of hydrogen over all loading materials tested is presented by means of hydrogen yield versus temperature. As expected, production of hydrogen when loading the reactor with sand, compared to the maximum possible for full reforming (reaction (5)), is very low, never surpassing 15%. As explained, the high selectivity in other hydrogen containing compounds in conjunction with the low C-to-gas conversion achieved is responsible for these low values. Olivine exhibited higher C-to-gas conversion, which in combination to the slightly lower selectivities in hydrocarbons, resulted in a maximum of 30% hydrogen yield. The presence of Ni on the surface is the key for the increase in hydrogen yield. At the lowest temperature tested, hydrogen yield exceeds 60% and reaches 80% at 850 °C, not far from the thermodynamic maximum.

As already demonstrated in sand and olivine tests, the favorable hydrodynamic characteristics of the spouted bed reactor help in minimizing coke production. On the other hand, the Ni/olivine system has been reported previously in literature [37] to possess noticeable anti-coking characteristics that were attributed to the formation of Ni–Fe alloys, known for increasing carbon-deposition resistance. The combination of these two beneficial features resulted in practically zero coke deposits during the catalytic runs (~0.02–0.07 wt% of the bed after 6 h TOS). Equally important to coke minimization, is resistance to attrition, a major problem for most fluidized bed applications. The Ni/olivine catalyst proved remarkably tolerant, similar to calcined olivine. Stable catalytic particles (after subjection to cold flow fluidization), exhibited very low percentage of weight losses due to abrasion during tests. As will be discussed in more detail in Section 4, it is believed that the process of cold flow spouting led to removal of a loosely linked NiO shell in the form of fines. At the same time, catalytic results prove that a percentage of Ni impregnated is strongly linked to the olivine structure, in agreement with previous reports [27,28]. The performance of the catalyst was stable throughout the period tested, requiring no reduction before experiments. To conduct all runs under common starting conditions, pretreatment of the catalyst with air at 800 °C was carried out.

In conclusion, the unique hydrodynamic features of the spouted bed reactor combined with the reforming activity, the low coking tendency and the attrition resistance of the Ni/olivine particles clearly demonstrate the prospects for successful processing of actual bio-oil at a commercial level.

4. Characterization of bed materials

4.1. Olivine

The specific surface area of the as received olivine was 3.02 m^2/g. Calcination at 1100 °C for 4 h resulted in a considerably lower area of 0.48 m^2/g, evident of the structural modifications inflicted. Fig. 8 shows X-ray diffractograms of natural olivine (a) and calcined olivine at 1100 °C (b) in the range of 26–46° 2θ, where the major peaks appear. All of the diffraction lines that are not identified in the figure correspond to those of forsterite Mg_2SiO_4, the major crystal phase of

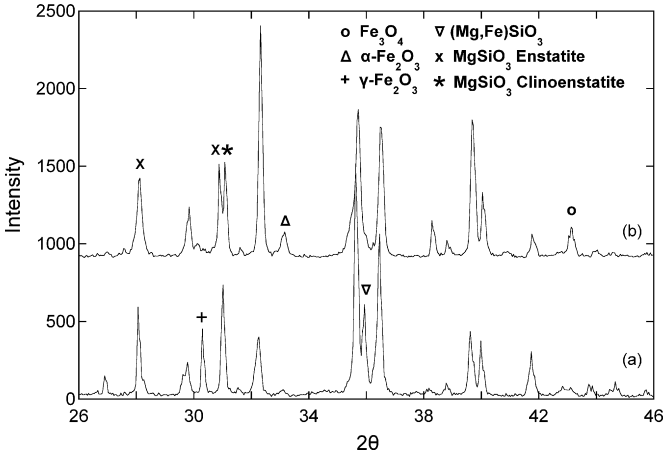

Fig. 8. X-ray diffractogram of (a) natural olivine and (b) calcined olivine at 1100 °C. The reflections without indications correspond to forsterite Mg_2SiO_4.

olivine. Secondary crystalline phases of natural olivine identified are enstatite $MgSiO_3$ at $2\theta = 28.1°$ and 31°, ferroan enstatite $(Mg,Fe)SiO_3$ at 35.95° and maghemite γ-Fe_2O_3 at 30.3°. After calcination of raw olivine at 1100 °C for 4 h the main olivine phase remains, but with modifications on line intensities. We can also observe the appearance of the hematite α-Fe_2O_3 reflection at $2\theta = 33.2°$ and magnetite Fe_3O_4 at 43.2° accompanied by the disappearance of the maghemite and ferroan enstatite reflections. Also noticeable is that due to the thermal treatment, part of enstatite changes to clinoenstatite as evident by the reflection at $2\theta = 31.1°$. The above observations are in agreement with those of Swierczynski et al. [34] who elaborated on the oxidation-reduction behavior of olivine. Maghemite γ-Fe_2O_3, observable in natural olivine, is a metastable phase explaining its disappearance after calcination. The presence of iron oxides was attributed by these authors to rejection of iron (Fe^{2+}) from the olivine structure due to its oxidation to Fe^{3+}, accompanied with the formation of amorphous silica and forsterite. This departure of iron from the structure of olivine is also responsible for the above indicated change in line intensities. As was mentioned

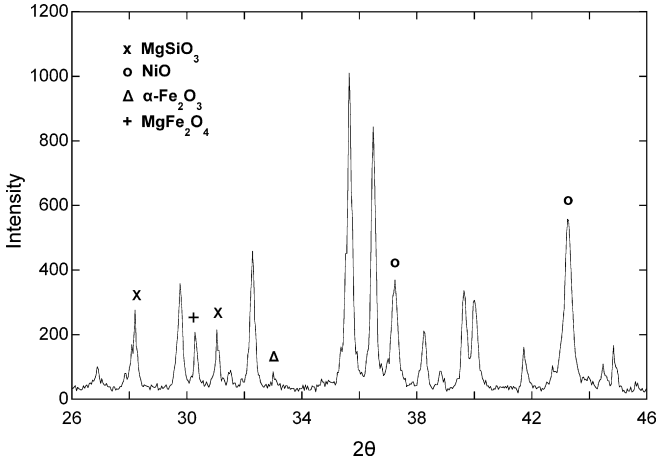

Fig. 9. X-ray diffractogram of Ni/olivine catalyst prior cold flow spouting. The reflections without indications correspond to forsterite Mg_2SiO_4.

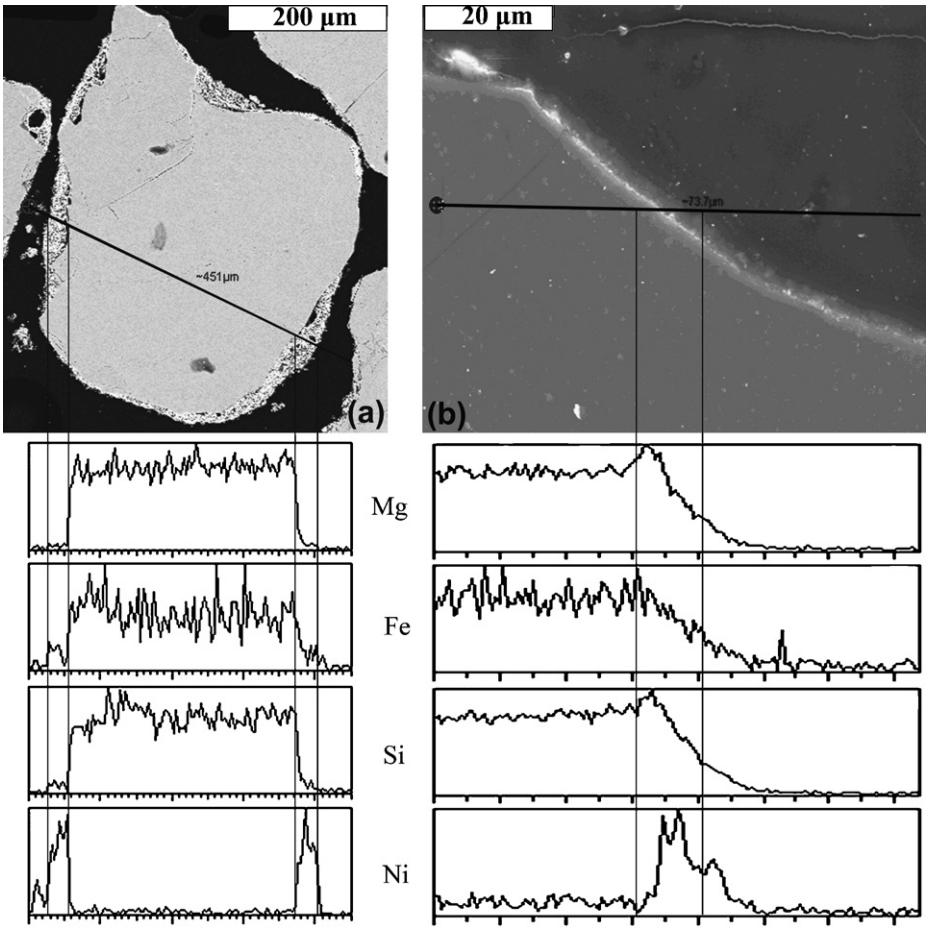

Fig. 10. SEM micrographs and EDS microanalysis on cut grains of Ni/olivine catalyst (a) before cold flow spouting and (b) after cold flow spouting.

previously, these oxides (α-Fe_2O_3 and Fe_3O_4) under reducing conditions, such as those encountered in a reforming reactor, can be reduced to some extent and are actually responsible for the cracking and reforming activity of olivine, as also evidenced in our experiments.

4.2. Ni/olivine catalyst

Fig. 9 presents the X-ray diffractogram of the fresh Ni/olivine prior cold flow spouting. When compared to natural olivine (Fig. 8a) we can see that the main olivine phase is retained. Differences lie on a change in the intensity of lines and in the appearance of nickel oxide at $2\theta = 37.25^\circ$ and 43.25°. The reflection of α-Fe_2O_3 at 33.2° is weak since calcination at 800 °C led to smaller percentage of iron rejection from olivine compared to 1100 °C, while the spinel phase at $2\theta = 30.3^\circ$ was identified as magnesioferrite $MgFe_2O_4$. By looking at SEM images and microanalysis on cut grains of the catalyst before and after cold flow spouting (Fig. 10a and b, respectively) we can understand better the effect of that treatment. An external shell covering catalyst particles before fluidization is easily observable in Fig. 10a. This layer as shown by EDS analysis is composed mainly of NiO, while the interior of the particle is pure olivine. The interaction of nickel oxide and olivine during calcination between 400 and 1400 °C was studied by Swierczynski et al. [37] who identified three different states: free NiO, NiO–MgO solid solution and nickel incorporated into olivine depending on temperature. The solid NiO–MgO solution was proposed as the most preferable interaction type, since that way nickel was strongly bound to olivine but was still reducible. At 800 °C (calcination temperature of our samples) the reaction between NiO and olivine leading to the NiO–MgO solid solution is slow and limited to the grain surface. As a result of cold flow spouting, the loosely bound NiO was removed. Fines created were, primarily, this loose NiO shell, together with some olivine mass. However, as seen from the SEM micrograph and EDS analysis of the resulting particles (Fig. 10b), a thin layer of nickel oxide (~10 μm) remains afterwards, which as proved from the experimental runs, is strongly linked to olivine. Taking into account the weight losses of the catalyst during cold flow spouting, the final Ni loading is around 1 wt%. The presence of even low amount of nickel on the surface of olivine is active enough to drive reforming reactions achieving hydrogen yield up to 80%.

5. Conclusions

The experimental work carried out in a novel spouted bed reactor for the reforming of ethylene glycol, a model compound of bio-oil, was presented. The implementation of the spouted bed

reactor configuration, modified by the use of a specially designed injection nozzle, was proven successful, resulting in efficient processing of the organic feed. Sand, olivine and a Ni/olivine catalyst were tested using ethylene glycol. Coke formation, a major problem encountered in most reforming processes, was drastically limited, regardless the particles tested, owing to the favorable hydrodynamics of the spouted bed. The rapid and effective mixing between the hot solid particles and the cold injected reactants minimizes coke generation. Ni/olivine appears to be a suitable catalytic system due to its high mechanical strength and anti-coking characteristics. Use of the catalyst resulted in the highest hydrogen yield of 80% at 850 °C and H_2O/C ratio equal to 4.6. Ni/olivine performance is attributed to strong nickel–olivine interactions developed during calcination. Further work on increasing the amount of strongly bound nickel to the olivine surface is in progress. The suitability of the reactor for the successful reforming of bio-oil will be further investigated by conducting tests in a wide range of operating conditions and model compounds of bio-oil and will conclude with the use of actual bio-oil.

Acknowledgements

Mrs. Vavaleskou T. from the Laboratory of Analysis and Characterization of Solids is acknowledged for her help with XRD and SEM measurements. Financial support was provided by GSRT-Programme PENED03.

References

[1] J.R. Rostrup-Nielsen, J. Sehested, J.K. Norskov, in: B.C. Gates, H. Knözinger (Eds.), Advances in Catalysis, vol. 47, Academic Press, 2002, p. 65.
[2] J. Piskorz, D.S. Scott, D. Radlein, Pyrolysis Oils from Biomass: Producing, Analyzing and Upgrading, American Chemical Society, Washington, DC, 1988.
[3] S. Czernik, D. Wang, D. Montane, E. Chornet, Developments in Thermochemical Biomass Conversion, Blackie Academic & Professional, London, 1997.
[4] M.C. Samolada, D.T. Patiaka, E. Grigoriadou, I.A. Vasalos, The Direct Catalytic Methylatation of the Phenolic Fraction of Biomass Flash Pyrolysis Liquids for the Production of Gasoline Blending Components, Pergamon, Oxford, 1994.
[5] S.S. Kelley, X.M. Wang, M.D. Myers, D.K. Johmson, J.W. Scahill, Developments in Thermochemical Biomass Conversion, Blackie, London, 1997.
[6] A.A. Iordanidis, P.N. Kechagiopoulos, S.S. Voutetakis, A.A. Lemonidou, I.A. Vasalos, Int. J. Hydrogen Energy 31 (2006) 1058.
[7] P.N. Kechagiopoulos, S.S. Voutetakis, A.A. Lemonidou, I.A. Vasalos, Energy Fuels 20 (2006) 2155.
[8] J.R. Galdamez, L. Garcia, R. Bilbao, Energy Fuels 19 (2005) 1133.
[9] M. Marquevich, S. Czernik, E. Chornet, D. Montane, Energy Fuels 13 (1999) 1160.
[10] D. Wang, S. Czernik, D. Montane, M. Mann, E. Chornet, Ind. Eng. Chem. Res. 36 (1997) 1507.
[11] D. Wang, D. Montane, E. Chornet, Appl. Catal. A Gen. 143 (1996) 245.
[12] A.C. Basagiannis, X.E. Verykios, Appl. Catal. A Gen. 308 (2006) 182.
[13] K. Takanabe, K.-i. Aika, K. Inazu, T. Baba, K. Seshan, L. Lefferts, J. Catal. 243 (2006) 263.
[14] K. Takanabe, K.-i. Aika, K. Seshan, L. Lefferts, Chem. Eng. J. 120 (2006) 133.
[15] S. Czernik, R. French, C. Feik, E. Chornet, Ind. Eng. Chem. Res. 41 (2002) 4209.
[16] L. Garcia, R. French, S. Czernik, E. Chornet, Appl. Catal. A Gen. 201 (2000) 225.
[17] C. Rioche, S. Kulkarni, M. Meunier, J. Breen, R. Burch, Appl. Catal. B Environ. 61 (2005) 130.
[18] D. Wang, S. Czernik, E. Chornet, Energy Fuels 12 (1998) 19.
[19] T. Davidian, N. Guilhaume, E. Iojoiu, H. Provendier, C. Mirodatos, Appl. Catal. B Environ. 73 (2007) 116.
[20] R.D. Cortright, R.R. Davda, J.A. Dumesic, Nature 418 (2002) 964.
[21] G.W. Huber, J.W. Shabaker, J.A. Dumesic, Science 300 (2003) 2075.
[22] G.W. Huber, J.W. Shabaker, S.T. Evans, J.A. Dumesic, Appl. Catal. B Environ. 62 (2006) 226.
[23] J. Corella, J.M. Toledo, R. Padilla, Energy Fuels 18 (2004) 713.
[24] L. Devi, M. Craje, P. Thne, K.J. Ptasinski, F.J.J.G. Janssen, Appl. Catal. A Gen. 294 (2005) 68.
[25] G. Hu, S. Xu, S. Li, C. Xiao, S. Liu, Fuel Process. Technol. 87 (2006) 375.
[26] C. Courson, E. Makaga, C. Petit, A. Kiennemann, Catal. Today 63 (2000) 427.
[27] C. Courson, L. Udron, C. Petit, A. Kiennemann, Sci. Technol. Adv. Mater. 3 (2002) 271.
[28] C. Courson, L. Udron, D. Swierczynski, C. Petit, A. Kiennemann, Catal. Today 76 (2002) 75.
[29] K.B. Mathur, N. Epstein, Spouted Beds, Academic Press Inc., New York, 1974.
[30] J. Dielbold, A Review of the Chemical and Physical Mechanisms of the Storage Stability of Fast Pyrolysis Bio-oils, Thermalchemie Inc., Lakewood, CO, 1999.
[31] P.J. Dauenhauer, J.R. Salge, L.D. Schmidt, J. Catal. 244 (2006) 238.
[32] E.C. Vagia, A.A. Lemonidou, Int. J. Hydrogen Energy 32 (2007) 212.
[33] L. Devi, K.J. Ptasinski, F.J.J.G. Janssen, Fuel Process. Technol. 86 (2005) 707.
[34] D. Swierczynski, C. Courson, L. Bedel, A. Kiennemann, S. Vilminot, Chem. Mater. 18 (2006) 897.
[35] S. Rapagna, N. Jand, A. Kiennemann, P.U. Foscolo, Biomass Bioenergy 19 (2000) 187.
[36] C. Wheeler, A. Jhalani, E.J. Klein, S. Tummala, L.D. Schmidt, J. Catal. 223 (2004) 191.
[37] D. Swierczynski, C. Courson, L. Bedel, A. Kiennemann, J. Guille, Chem. Mater. 18 (2006) 4025.